MODEL DISTRIBUTION FOR DISTRIBUTED KALMAN FILTERS: A GRAPH THEORETIC APPROACH

Usman A. Khan and José M. F. Moura

Department of Electrical and Computer Engineering
Carnegie Mellon University, Pittsburgh, PA 15213
{ukhan, moura}@ece.cmu.edu

ABSTRACT

This paper discusses the distributed Kalman filter problem for the state estimation of sparse large-scale systems monitored by sensor networks. With limited computing resources at each sensor, no sensor has the ability to replicate locally the entire large-scale state-space model. We investigate techniques to *distribute* the model, i.e., to have at each sensor low-dimensional coupled local models that are computationally viable and provide accurate representation of the local states. We implement local Kalman filters over these coupled reduced models. We use system digraphs and cut-point sets for model distribution. Under certain conditions, the local Kalman filters asymptotically guarantee the performance of the centralized Kalman filter.

1. INTRODUCTION

Large-scale integration in sensing and communication technologies has made possible for sensor networks to monitor sparse large-scale dynamical systems, e.g., electric power systems, water management systems, gas-pipeline systems, or weather forecast systems. State estimation is necessary for control, tracking and navigational purposes. Due to their large geographical span and their high dimensionality, centralized state estimation schemes are challenged with inordinate communication and computational needs. These can be avoided if the system can be distributed into smaller coupled systems by exploiting the sparsity and locality inherent in the system structure. Local estimation schemes can be employed on these low-dimensional systems and information exchange among them is used to achieve performance equivalent to the performance of a centralized scheme.

We study Kalman filters for the purpose of state estimation. Several studies have been conducted to distribute the Kalman filter implementation, but they have practical limitations when it comes to large-scale systems. These include decentralizing the Kalman filter observation equations so that the distributed sensor observations are not collected at a central location [1, 2, 3] and implementing local Kalman filters based on reduced-order models [4, 5] so that the computational requirements can be decreased. The former, [1, 2, 3], involve computations with nth order vectors and matrices (where n is the dimension of the state vector), which is infeasible when n is extremely large as may be the case in large-scale systems. The latter, [4, 5], decouples the global model of the large-scale system into decoupled reduced-order models. This decoupling ignores relevant correlation information among the states. Furthermore, sparse and localized structures that underlie the system dynamics are also not taken into account. Localized refers to model matrices in which the coupling between states that are farther apart in the state vector decays in an appropriate measure. Localized model matrices include, but are not limited to, banded matrices. Banded matrices arise many times as a result of discretizing random fields governed by partial differential equations.

We present a completely decentralized solution where all the sensor observations are never collected at the same location, and, where only low order computations are implemented. This requires the global model to be distributed into reduced-order models (so that the computations required at each sensor are reduced), keeping the coupling among these reduced models intact. We use the Information filter [5], algebraically equivalent to the Kalman filter [6], for the purposes of state estimation. In this paper, we distribute the global model of the large-scale system into coupled sensor-based reduced models by exploiting the inherent physical structure of such systems. We can then implement local Information filters on these sensor-based models. We achieve the decentralization by only collecting the relevant sensor observations pertinent to the local Information filter at that sensor. We take into account the coupling between the reduced models through information exchange among the local Information filters.

The model distribution we present here exploits the spatial structure of the large-scale systems. We provide a top-down approach for spatially decomposing a large-scale system in which the large-scale model dynamics are already fixed. A bottom-up approach, where several local systems have fixed model dynamics but the coupling topology among these local systems can be chosen is studied in [7]. An important question in this bottom-up setup is the following: under what topological constraints on the coupling among local systems do the local estimation procedures remain optimal and track the global performance. The top-down approach that we study has a fixed dynamical topology for the large-scale systems. The notion of local systems is not apparent in this scenario and several different local systems can be chosen. We provide a sensor-based approach to choose the local systems. Once the local systems are chosen, the coupling topology among the local systems is fixed as given by the large-scale model dynamics, which we cannot alter.

As an example, consider figure 1 where a large-scale system with arbitrary dynamics is shown. The circles are the state variables and the arrows among the state variables show the coupling between them. Figure 2 shows the local systems implemented on the dynamical system in figure 1 as larger (red) ovals. The local systems are selected one at each sensor and they include all the states that the

This work was partially supported by the DARPA DSO Advanced Computing and Mathematics Program Integrated Sensing and Processing (ISP) Initiative under ARO grant # DAAD 19-02-1-0180, by NSF under grants # ECS-0225449 and # CNS-0428404, by ONR under grant # MURI-N000140710747, and by an IBM Faculty Award.

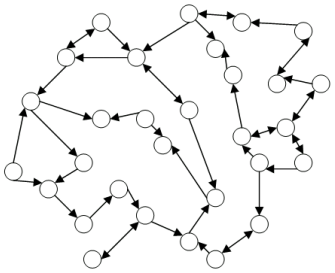

Fig. 1. Arbitrary dynamical system: the state variables represented by circles and the interconnections among them represent their coupling.

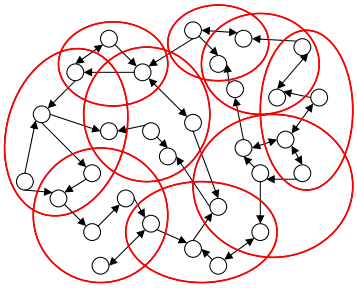

Fig. 2. Sensor-based local systems are implemented on the arbitrary large-scale dynamical system shown in figure 1.

sensors observe (directly or indirectly[1]). We assume here, without loss of generality, that each state is observed (directly or indirectly) at least at one sensor. The coupling topology among the local systems in figure 2 is now defined by the dynamics of the large-scale system: there is an edge among the local systems if the states they include have an interconnection.

Since the local systems are coupled, the local Information filters implemented on them are also coupled. It can be shown that due to this coupling the local error covariance matrix at each local system is a function of the global error covariance matrix, see [8]. Hence, a distributed procedure to compute the global error covariance matrix is required. To achieve this, while preserving the locality of the computations, we approximate the information matrices, inverse of the error covariance matrices, to be L-banded. This approximation is equivalent to forcing the Gaussian error processes in the Kalman filter to be Lth order Gauss-Markovian [9] processes and is optimal in Kullback-Leibler sense [10]. These approximations enable us going from the local variables to the appropriate submatrices/subvectors in the global variables through only local communication involving only local variables. Implementing the centralized Information filter with these approximations is shown to be practically indistinguishable from the exact scheme in [11].

This paper explains how to achieve model distribution using system digraphs and cut-point sets in section 3 from the global model representing the large-scale system presented in section 2. Section 2 also presents the centralized Information filter. A summary of the steps required in implementing local Information filters is provided in section 4. Section 5 presents simulation results and section 6 concludes the paper.

[1]If a sensor observes a linear combination of some states, these states are said to be observed indirectly by the corresponding sensor.

2. GLOBAL MODEL

The global model assumed is the discrete time state-space representation given by

$$\mathbf{x}_{k+1} = \mathbf{F}\mathbf{x}_k + \mathbf{G}\mathbf{u}_k, \qquad k \geq 0, \tag{1}$$

where: $\mathbf{x}_k$ is the n-dimensional state; $\mathbf{F}$ is the model matrix; $\mathbf{u}_k \sim \mathscr{N}(\mathbf{0}, \mathbf{Q})$ is the white noise input vector; $\mathbf{x}_0 \sim \mathscr{N}(\overline{\mathbf{x}}_0, \mathbf{\Sigma_0})$ are the initial conditions. We have N sensors observing the random field in (1). The p_l-dimensional observation vector for the lth sensor is given by

$$\mathbf{y}_k^{(l)} = \mathbf{H}_l\mathbf{x}_k + \mathbf{w}_k^{(l)}, \tag{2}$$

where $\mathbf{H}_l$ is the local observation matrix with the white observation noise vector $\mathbf{w}_k^{(l)} \sim \mathscr{N}(0, \mathbf{R}_l)$.

We stack the local observations to get the global observation vector,

$$\mathbf{y}_k = \begin{bmatrix} \mathbf{y}_k^{(1)} \\ \vdots \\ \mathbf{y}_k^{(N)} \end{bmatrix}, \quad \mathbf{H} = \begin{bmatrix} \mathbf{H}_1 \\ \vdots \\ \mathbf{H}_N \end{bmatrix}, \quad \mathbf{w}_k = \begin{bmatrix} \mathbf{w}_k^{(1)} \\ \vdots \\ \mathbf{w}^{(N)} \end{bmatrix}. \tag{3}$$

The global observation model is

$$\mathbf{y}_k = \mathbf{H}\mathbf{x}_k + \mathbf{w}_k. \tag{4}$$

The noise sequences $\{\mathbf{u}\}_{k\geq 0}$ and $\{\mathbf{w}\}_{k\geq 0}$ and the initial condition, $\mathbf{x}_0$, are all statistically independent. Furthermore, the local observation noise vectors are uncorrelated among the sensors and we can write $\mathbf{R} = \text{blockdiag}[\mathbf{R}_1, \mathbf{R}_2, ..., \mathbf{R}_N]$. We assume that the global state-space dynamical and observation model, given by (1) and (4), is $(\mathbf{F}, \mathbf{H})-$observable.

Centralized Information Filter: In this version of the Kalman filter, the state estimate, $\widehat{\mathbf{x}}_{k|k}$, and predictor, $\widehat{\mathbf{x}}_{k|k-1}$, are transformed as $\widehat{\mathbf{z}}_{k|k} = \mathbf{Z}_{k|k}\widehat{\mathbf{x}}_{k|k}$, and $\widehat{\mathbf{z}}_{k|k-1} = \mathbf{Z}_{k|k-1}\widehat{\mathbf{x}}_{k|k-1}$, respectively, where the information matrices, $\mathbf{Z}_{k|k}$, and $\mathbf{Z}_{k|k-1}$, are the inverses of the estimation error covariance matrix, $\mathbf{S}_{k|k}$, and prediction error covariance matrix, $\mathbf{S}_{k|k-1}$, respectively. Let $\mathbf{i}_k = \mathbf{H}^T\mathbf{R}^{-1}\mathbf{y}_k$ and $\mathbf{I}_k = \mathbf{H}^T\mathbf{R}^{-1}\mathbf{H}$. It is straightforward to write, [1, 5]

$$\mathbf{i}_k = \sum_{l=1}^{N} \mathbf{H}_l^T\mathbf{R}_l^{-1}\mathbf{y}_k^{(l)}, \tag{5}$$

$$\mathbf{I}_k = \sum_{l=1}^{N} \mathbf{H}_l^T\mathbf{R}_l^{-1}\mathbf{H}_l. \tag{6}$$

The centralized Information filter equations for the global model (1) and (4) are given by: initial conditions $\mathbf{Z}_{0|-1} = \mathbf{\Sigma}_0^{-1}$ and $\widehat{\mathbf{z}}_{0|-1} = \mathbf{Z}_{0|-1}\overline{\mathbf{x}}_0$, a filter step (7), and a prediction step (8).

$$\mathbf{Z}_{k|k} = \mathbf{Z}_{k|k-1} + \sum_{l=1}^{N} \mathbf{H}_l^T\mathbf{R}_l\mathbf{H}_l \tag{7a}$$

$$\widehat{\mathbf{z}}_{k|k} = \widehat{\mathbf{z}}_{k|k-1} + \sum_{l=1}^{N} \mathbf{H}_l^T\mathbf{R}_l\mathbf{y}_k^{(l)} \tag{7b}$$

$$\mathbf{Z}_{k|k-1} = (\mathbf{F}\mathbf{Z}_{k-1|k-1}^{-1}\mathbf{F}^T + \mathbf{G}\mathbf{Q}\mathbf{G}^T)^{-1} \tag{8a}$$

$$\widehat{\mathbf{z}}_{k|k-1} = \mathbf{Z}_{k|k-1}\left(\mathbf{F}\mathbf{Z}_{k-1|k-1}^{-1}\widehat{\mathbf{z}}_{k-1|k-1}\right) \tag{8b}$$

3. MODEL DISTRIBUTION USING SYSTEM DIGRAPHS

We distribute the global model (1) and (4) to derive coupled low-dimensional local models. With low-dimensional models, we can implement local low-order Information filters at each sensor that are computationally efficient. The coupling among the local models is preserved through information exchange among the local Information filters. We illustrate the procedure of model distribution using an example. Consider a 5-dimensional system with $N = 3$ sensors.

$$\begin{aligned}\mathbf{x}_{k+1} &= \begin{bmatrix} f_{11} & 0 & f_{13} & 0 & 0 \\ f_{21} & f_{22} & 0 & f_{42} & 0 \\ f_{31} & 0 & f_{33} & 0 & 0 \\ 0 & 0 & f_{43} & 0 & f_{45} \\ 0 & 0 & 0 & f_{54} & f_{55} \end{bmatrix} \mathbf{x}_k \\ &+ \begin{bmatrix} 0 & g_{12} \\ 0 & 0 \\ 0 & 0 \\ 0 & 0 \\ g_{51} & 0 \end{bmatrix} \mathbf{u}_k \\ &= \mathbf{F}\mathbf{x}_k + \mathbf{G}\mathbf{u}_k. \end{aligned} \tag{9}$$

$$\begin{aligned}\mathbf{y}_k = \begin{bmatrix} y_k^{(1)} \\ y_k^{(2)} \\ y_k^{(3)} \end{bmatrix} &= \begin{bmatrix} h_{11} & h_{12} & 0 & 0 & 0 \\ 0 & h_{22} & h_{23} & h_{24} & 0 \\ 0 & 0 & 0 & h_{34} & h_{35} \end{bmatrix} \mathbf{x}_k \\ &+ \begin{bmatrix} w_k^{(1)} \\ w_k^{(2)} \\ w_k^{(3)} \end{bmatrix} \\ &= \mathbf{H}\mathbf{x}_k + \mathbf{w}_k, \end{aligned} \tag{10}$$

where $\mathbf{H} = [\mathbf{H}_1^T, \mathbf{H}_2^T, \mathbf{H}_3^T]^T$. Equations (9) and (10) comprise the *global model* for our example, which we will distribute by formulating reduced order models with the help of system digraphs and cut-point sets as follows.

A system digraph [7], $J = [V, E]$, is a directed graphical representation of the system, where V is the vertex set that contains the states, $\{x_i\}$, and the inputs, $\{u_i\}$, of the system, and E is the edge matrix or the interconnection matrix of the system. The interconnection matrix, E, for the system in (9) is,

$$E = \begin{bmatrix} 1 & 0 & 1 & 0 & 0 & 0 & 1 \\ 1 & 1 & 0 & 1 & 0 & 0 & 0 \\ 1 & 0 & 1 & 0 & 0 & 0 & 0 \\ 0 & 0 & 1 & 0 & 1 & 0 & 0 \\ 0 & 0 & 0 & 1 & 1 & 1 & 0 \end{bmatrix}, \tag{11}$$

which is sparse, reflecting the system structure. The system digraph is shown in figure 3 with black solid lines.

Each sensor l corresponds to a *cut-point set* $\mathbf{V}^{(l)}$ [12], which contains a state variable, x_i, if the corresponding sensor observes x_i directly or indirectly. Hence, the cut-point sets extract the state variables relevant to the local dynamics at each sensor. From (10), we have the following cut-point set at sensor 1,

$$V^{(1)} = [x_1, x_2]. \tag{12}$$

The cut-point sets corresponding to this and the other two sensors are shown in figure 3. We chose in this example that each state variable is observed by at least one sensor. We are not restricted to this choice.

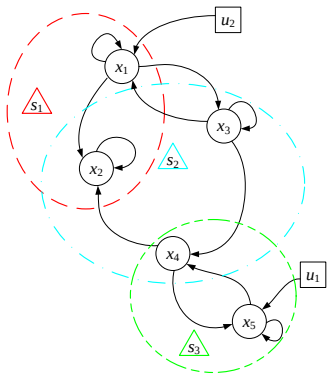

Fig. 3. The system digraph of the 5 dimensional system, (9)-(10) is shown as black solid lines, where the circles represent the states, $\mathbf{x}$, of the system, and the squares represent the input noise sources, $\mathbf{u}$. The cut-point sets associated to the 3 sensors ($\triangle$) are shown in dotted (colored) circles.

The local states at sensor l, $\mathbf{x}_k^{(l)}$, are the vertices in its associated cut-point set, $V^{(l)}$. The local state vector, $\mathbf{x}_k^{(l)}$, is coupled to the other reduced models through the arrows coming into $V^{(l)}$, see figure 3. The states that are coupled to $\mathbf{x}_k^{(l)}$ are the inputs required to the local model at sensor l. The inputs are collected in a local input vector, $\mathbf{d}_k^{(l)}$. The coupling coefficients are the corresponding terms to the inputs, $\mathbf{d}_k^{(l)}$, in the model matrix, $\mathbf{F}$, and are collected in the local input matrix $\mathbf{D}^{(l)}$. The local model matrix, $\mathbf{F}^{(l)}$, corresponds to the local state vector, $\mathbf{x}_k^{(l)}$. This partitioning gives us the following reduced sensor-based model at sensor 1

$$\begin{aligned}\mathbf{x}_{k+1}^{(1)} &= \begin{bmatrix} f_{11} & 0 \\ f_{21} & f_{22} \end{bmatrix} \mathbf{x}_k^{(1)} \\ &+ \begin{bmatrix} f_{13} & 0 \\ 0 & f_{24} \end{bmatrix} \begin{bmatrix} x_{3,k} \\ x_{4,k} \end{bmatrix} + \begin{bmatrix} g_{12} \\ 0 \end{bmatrix} u_{2,k}, \\ &= \mathbf{F}^{(1)}\mathbf{x}_k^{(1)} + \mathbf{D}^{(1)}\mathbf{d}_k^{(1)} + \mathbf{G}^{(1)}\mathbf{u}_k^{(1)} \end{aligned} \tag{13}$$

Since $\mathbf{F}$ is sparse, there are only a few interconnections among the reduced models. If $\mathbf{F}$ is localized, the interconnections are from neighboring sensors and thus long-distance communication links can be avoided. The reduced local observation model is obtained by retaining only the terms corresponding to $\mathbf{x}_k^{(l)}$ in $\mathbf{H}_l$, and for sensor 1 is given by

$$\mathbf{y}_k^{(1)} = \mathbf{H}^{(1)}\mathbf{x}_k^{(1)} + \mathbf{w}_k^{(1)}, \tag{14}$$

where $\mathbf{H}^{(1)} = [h_{11}\ h_{12}]$. The coupled state vector, $\mathbf{d}_k^{(l)}$, associated to a reduced model is unavailable. We use its estimate, $\widehat{\mathbf{d}}_{k|k}^{(l)}$, to account for the coupled information among the reduced models[2]. Generalizing to an arbitrary sensor l, we have the following reduced model.

$$\mathbf{x}_{k+1}^{(l)} = \mathbf{F}^{(l)}\mathbf{x}_k^{(l)} + \mathbf{D}^{(l)}\widehat{\mathbf{d}}_{k|k}^{(l)} + \mathbf{G}^{(l)}\mathbf{u}_k^{(l)} \tag{15}$$

$$\mathbf{y}_k^{(l)} = \mathbf{H}^{(l)}\mathbf{x}_k^{(l)} + \mathbf{w}_k^{(l)} \tag{16}$$

[2]The procedure of choosing the cut-point sets is different from [12]. Furthermore, the notion of estimated inputs to a particular reduced model is novel in this approach.

4. LOCAL INFORMATION FILTERS

The local Information filters are based on the reduced sensor-based models (15) and (16). Since these reduced models may have shared states as it is clear from the overlapped cut-point sets in figure 3, different observations of these shared states made by different sensors should be fused in order to achieve the centralized performance [13]. It is shown in [13] that observation fusion for local Information filters only requires a particular subset of observations available at the neighboring sensors and thus involves only local communication and computations involving reduced variables. With the observation fusion, the *local filter step* of the local Information filters is given by

$$\mathbf{Z}_{k|k}^{(l)} = \mathbf{Z}_{k|k-1}^{(l)} + \mathbf{I}_{f,l,k}, \quad (17a)$$

$$\widehat{\mathbf{z}}_{k|k}^{(l)} = \widehat{\mathbf{z}}_{k|k-1}^{(l)} + \mathbf{i}_{f,l,k}, \quad (17b)$$

where $\mathbf{I}_{f,l,k}$ and $\mathbf{i}_{f,l,k}$ represent the fused observations at sensor l and time k.

Gauss-Markovian Approximation of the Error Processes: The Gaussian error processes of the Kalman filter, given by

$$\epsilon_{k|k} = \mathbf{x}_k - \widehat{\mathbf{x}}_{k|k}, \quad (18)$$

$$\epsilon_{k|k-1} = \mathbf{x}_k - \widehat{\mathbf{x}}_{k|k-1}, \quad (19)$$

are completely characterized by their $n \times n$ covariance matrices, $\mathbf{S}_{k|k}$ and $\mathbf{S}_{k|k-1}$. Preserving these covariance matrices among the local Information filters requires $O(n^3)$ computation and $O(n^2)$ storage at each sensor. This violates our requirement of a low-order computational scheme. To overcome this, we approximate the Gaussian error processes to be Lth order Gauss-Markovian. This is equivalent to approximating the information matrices, $\mathbf{Z}_{k|k}$ and $\mathbf{Z}_{k|k-1}$, inverse of the error covariance matrices, to be $L-$banded[3], see [9], and is optimal in Kullback-Leibler or maximum entropy sense, see [10].

With the Gauss-Markovian approximation on the error processes, their $n \times n$ covariance matrices, $\mathbf{S}_{k|k}$ and $\mathbf{S}_{k|k-1}$, are completely characterized by their $L-$band. Any non $L-$band element of a matrix whose inverse is $L-$banded can be written as a function of the elements inside the $L-$band, see [11]. Thus, preserving the Gauss-Markovian error structure is equivalent to preserving the $L-$band of the error covariance matrices, $\mathbf{S}_{k|k}$ and $\mathbf{S}_{k|k-1}$. With this approximation, we proceed further with the local Information filters as follows.

The filtered estimates, $\widehat{\mathbf{z}}_{k|k}^{(l)}$, are converted to estimates in the Kalman filter domain, $\widehat{\mathbf{x}}_{k|k}^{(l)}$, by solving the linear systems of equations for banded matrices, $\mathbf{Z}_{k|k}\widehat{\mathbf{x}}_{k|k} = \widehat{\mathbf{z}}_{k|k}$, using a special case of the distributed iterate-collapse inversion (DICI) algorithm [14], which requires only local communication and processes local matrices.

It can be shown [8], that the local error covariance matrix is given by

$$\mathbf{S}_{k|k-1}^{(l)} = \mathbf{F}_l \mathbf{S}_{k-1|k-1} \mathbf{F}_l^T + \mathbf{G}^{(l)} \mathbf{Q}^{(l)} \mathbf{G}^{(l)T}, \quad (20)$$

where $\mathbf{F}_l$ is the $n_l \times n$ submatrix of the model matrix, $\mathbf{F}$, with n_l rows of $\mathbf{F}$ that correspond to the n_l local states at sensor l. From the sparse and localized global model matrix, $\mathbf{F}$, the submatrices local to sensor l are $\mathbf{F}^{(l)}$ and $\mathbf{D}^{(l)}$, as shown in (15). It can be shown [8], that (20) is equivalent to

$$\begin{aligned}\mathbf{S}_{k|k-1}^{(l)} &= \mathbf{F}^{(l)} \mathbf{S}_{k-1|k-1}^{(l)} \mathbf{F}^{(l)T} + \mathbf{F}^{(l)} \mathbf{S}_{k-1|k-1}^{(q)} \mathbf{D}^{(l)T} \\ &+ \left(\mathbf{F}^{(l)} \mathbf{S}_{k-1|k-1}^{(q)} \mathbf{D}^{(l)T}\right)^T + \mathbf{D}^{(l)} \mathbf{S}_{k-1|k-1}^{(v)} \mathbf{D}^{(l)T} \\ &+ \mathbf{G}^{(l)} \mathbf{Q}^{(l)} \mathbf{G}^{(l)T}, \end{aligned} \quad (21)$$

which requires submatrices ($\mathbf{S}_{k-1|k-1}^{(\cdot)}$) in the global estimation error covariance matrix, $\mathbf{S}_{k-1|k-1}$, from the neighboring sensors v and q. To go from the local estimate information matrix, $\mathbf{Z}_{k-1|k-1}^{(l)}$, provided by the local filter step (17a), to the submatrices in the global estimation error covariance matrix, $\mathbf{S}_{k-1|k-1}^{(\cdot)}$, and hence compute (21), we use the distributed iterate-collapse inversion (DICI) algorithm presented in [14, 8]. The local prediction error covariance matrix, $\mathbf{S}_{k|k-1}^{(l)}$, is inverted to get local prediction information matrix, $\mathbf{Z}_{k|k-1}^{(l)}$, using the L-banded inversion theorem [10]. Finally, along with (21), the *local prediction step* is completed by, see [8]

$$\begin{aligned}\widehat{\mathbf{z}}_{k|k-1}^{(l)} &= \mathbf{Z}_{k|k-1}^{(l)} \left(\mathbf{F}^{(l)} \widehat{\mathbf{x}}_{k-1|k-1}^{(l)} + \mathbf{D}^{(l)} \widehat{\mathbf{d}}_{k-1|k-1}^{(l)}\right) \\ &+ f_1\left(\mathbf{Z}_{k|k-1}^{(\mathcal{V})}, \mathbf{F}^{(\mathcal{V})}, \widehat{\mathbf{x}}_{k-1|k-1}^{(\mathcal{Q})}\right), \end{aligned} \quad (22)$$

for some $\mathcal{V}, \mathcal{Q}$, neighbors of sensor l, and where $f_1(\cdot)$ is a linear function that depends on L.

The local Information filter is given by the equations (17)-(22). It can be noted that nowhere in these equations an nth order variable is required, i.e., all the variables involved are local to the sensors.

5. SIMULATION RESULTS

We simulate the $n = 5-$dimensional system presented in (9)–(10) monitored by $N = 3$ sensors. We implement the local Information filters with $L = 1-$banded approximation on the information matrices, $\mathbf{Z}_{k|k}$ and $\mathbf{Z}_{k|k-1}$. Figure 4 and figure 5 show the trace of the error covariance matrix, $\mathbf{S}_{k|k}$, plotted against the Information filter iterations. Figure 4 compares the optimal Information filter performance with centralized Information filter with $L = 2-$banded approximation averaged over 1000 Monte-Carlo simulations. The solution of the Riccati equation is also shown in figure 4. Figure 5 compares the trace of the error covariance matrix, $\mathbf{S}_{k|k}$, for the centralized $L = 1-$banded Information filter and the local $L = 1-$banded Information filters averaged over 1000 Monte-Carlo simulations. The local models have the dimensions $n_l = 2, 3, 2$, smaller than $n = 5$. Figure 6 shows the estimates of the local $L = 1-$banded Information filters and the optimal Information filter estimates along with the state variables.

6. CONCLUSIONS

From the simulation results, we deduce the following conclusions. As $L \uparrow$, $L-$banded Information filters converge to the optimal Information filter, as shown in figure 4. The local $L-$banded Information filters asymptotically converge to the centralized $L-$banded Information filter. In figure 5, the performance of the local scheme is exactly the same as that of the the centralized $L-$banded scheme. The estimates in figure 6 are virtually indistinguishable from the optimal estimates. The steady state error for $L = 1-$banded approximation is considerably removed when $L \uparrow$.

[3]We refer to a matrix as an L-banded matrix ($L \geq 0$), if the elements outside the band defined by the Lth upper and Lth lower diagonal are zero.

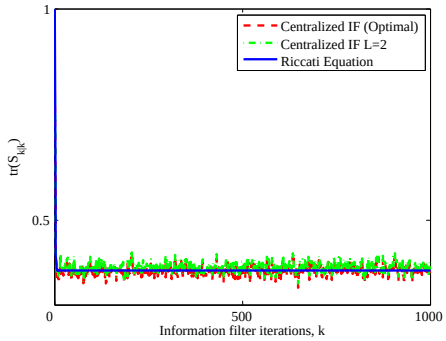

Fig. 4. Trace of the error covariance matrix, $\mathbf{S}_{k|k}$, is plotted for the centralized optimal Information filter and centralized $L = 2-$banded Information filter. The solution to the Riccati equation is also shown.

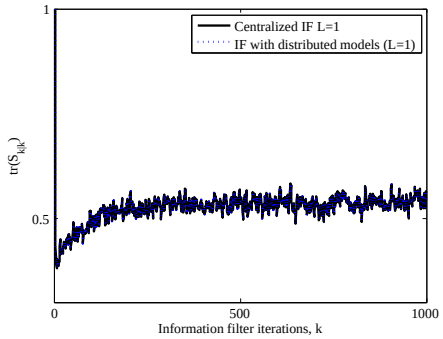

Fig. 5. Trace of the error covariance matrix, $\mathbf{S}_{k|k}$, is plotted for the centralized $L = 1-$banded Information filter and local $L = 1-$banded Information filters.

We presented a distributed implementation of the Kalman filter for large-scale systems when the exact centralized filter is practically infeasible. The local scheme we proposed approximates the filter error processes in the Kalman filter by Gauss-Markov processes. The local scheme asymptotically guarantees the performance of the centralized filter with the same Gauss-Markovian approximation of the error processes. To derive the distributed filter, we spatially decompose the large-scale system dynamics into coupled low-order local dynamical systems. Local Information filters are implemented on the low-order models and centralized performance is guaranteed through information exchange among the local Information filters. The proposed scheme has significant computational advantages as compared to the centralized optimal solution and thus provides a practically viable implementation.

7. REFERENCES

[1] B. Rao and H. Durrant-Whyte, "Fully decentralized algorithm for multisensor Kalman filtering," *IEE Proceedings-Control Theory and Applications*, vol. 138, pp. 413–420, Sep. 1991.

[2] R. Olfati-Saber, "Distributed Kalman filters with embedded consensus filters," in *44th IEEE Conference on Decision and Control*, Seville, Spain, Dec. 2005, pp. 8179 – 8184.

[3] M. Alanyali and V. Saligrama, "Distributed tracking in multi-hop networks with communication delays and packet losses," in *13th IEEE Workshop on Statistical Sig. Proc.*, Bordeaux, France, Jul. 2005, pp. 1190–1195.

[4] T. Berg and H. Durrant-Whyte, "Model distribution in decentralized multi-sensor data fusion," Tech. Rep., University of Oxford, 1990.

[5] A. Mutambara, *Decentralized estimation and control for multisensor systems*, CRC Press, Boca Raton, FL, 1998.

[6] R. Kalman, "A new approach to linear filtering and prediction problems," *Trans. of the ASME - Journal of Basic Engineering*, vol. 82, no. 2, pp. 35–45, 1960.

[7] Dragoslav Šiljak, *Decentralized control of complex systems*, Academic Press Inc., Boston, MA, 1991.

[8] Usman A. Khan and José M. F. Moura, "Distributing the Kalman filters for large-scale systems," Submitted to IEEE Trans. on Signal Processing, http://arxiv.org/pdf/0708.0242, Aug. 2007.

[9] N. Balram and José M. F. Moura, "Noncausal Gauss Markov random fields: Parameter structure and estimation," *IEEE Trans. on Information Theory*, vol. 39, no. 4, pp. 1333–1355, Jul. 1993.

[10] A. Kavcic and José M. F. Moura, "Matrices with banded inverses: Inversion algorithms and factorization of Gauss-Markov processes," *IEEE Trans. on Information Theory*, vol. 46, no. 4, pp. 1495–1509, Jul. 2000.

[11] A. Asif and José M. F. Moura, "Inversion of block matrices with L-block banded inverse," *IEEE Trans. on Sig. Proc.*, vol. 53, no. 2, pp. 630–642, Feb. 2005.

[12] H. Zhang, José M. F. Moura, and B. Krogh, "Estimation in sensor networks: A graph approach," in *4th International Symposium on Information Processing in Sensor Networks*, Los Angeles, CA, Apr. 2005, pp. 203–209.

[13] Usman A. Khan and José M. F. Moura, "Distributed Kalman filters in sensor networks: Bipartite fusion graphs," in *15th IEEE Workshop on Statistical Sig. Proc.*, Madison, WI, Aug. 26-29 2007, pp. 700–704.

[14] Usman A. Khan and José M. F. Moura, "Distributed Iterate-Collapse inversion (DICI) algorithm for $L-$banded matrices," in *33rd International Conference on Acoustics, Speech, and Signal Processing*, Las Vegas, NV, Mar 30-Apr 04 2008, submitted.

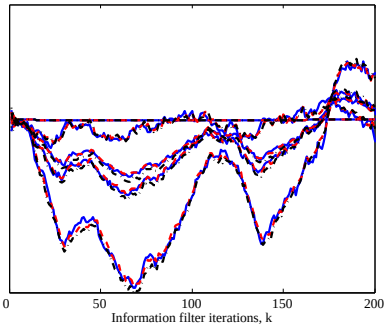

Fig. 6. Local $L = 1-$banded Information filter estimates (black/dash-dot) are compared to the optimal estimates (red/dashed) and the actual states (blue/solid).